





High-throughput-generating water-in-water droplet for monodisperse biocompatible particle synthesis

Qingquan Zhang¹ , Jiaqu Chen¹, and Hongwei Gai^{1,*} 

¹ Jiangsu Key Laboratory of Green Synthesis for Functional Materials, School of Chemistry and Materials Science, Jiangsu Normal University, Xuzhou 221116, Jiangsu, China

Received: 8 July 2019

Accepted: 4 September 2019

Published online:

9 September 2019

© Springer Science+Business Media, LLC, part of Springer Nature 2019

ABSTRACT

Water-in-water (W/W) droplets are biocompatible vessels for bioanalysis and biomolecules delivery. Due to the ultralow interfacial tension, the stable generation of W/W droplets still faces some challenges. In this paper, we present a robust and high-throughput microfluidic platform to fabricate W/W droplets without requiring external perturbation. Using the assembled evaporation pump, W/W droplets are generated uniformly and stably for nearly 1 h. The molecular weights, concentrations, and flow rates were changed to regulate the droplet size in the range of 44–93 μm . The production of droplets is scaled up by parallelizing eight droplet-formation units on a 3-D microdevice, and the variable coefficient of droplet size in all units reaches 3.2%. Using these W/W droplets as microreactors, monodispersed hydrogel particles are synthesized by either UV light or calcium ions, and recovered conveniently without cumbersome post-processing. The established method is simple, robust and suitable for various aqueous two-phase systems, displaying its potential in biocompatible carrier synthesis.

Introduction

Water-in-water (W/W) droplets are generally formed by two incompatible polymer solutions, or a polymer solution and certain salts solution [1]. In contrast to water-in-oil (W/O) system, W/W droplets contain no organic phase and possess some unique advantages [2]: (1) providing a high biocompatible environment to protect cells/biomolecules from degradation or

denaturation; (2) recovering target samples easily from continuous phase and not requiring expensive and cumbersome post-processing; (3) discharging environmentally digestible continuous phase without professional treatments [3]. Considering these properties, W/W droplets have been widely applied in colloidosomes fabrication [4, 5], biomolecules delivery [6, 7], and single-cell encapsulation [8].

In a microfluidic chip, droplet formation depends on the Rayleigh–Plateau instability when a liquid jet

Qingquan Zhang and Jiaqu Chen have contributed equally to this work.

Address correspondence to E-mail: gai@jsnu.edu.cn

<https://doi.org/10.1007/s10853-019-04001-w>

is introduced into another immiscible phase [1]. For the W/O system, the relatively high interfacial tension (1–40 mN/m) enables rapid growth of the Rayleigh–Plateau instability and ensures the stable breakup of droplets [9]. However, the interfacial tension in the W/W system is often less than 0.1 mN/m, which induces a very slow growth of the Rayleigh–Plateau instability along the jet [10]. A liquid thread may survive throughout the channel, or non-uniform droplets are generated far downstream [11]. In order to generate W/W droplets stably, various external forces are used to promote the breakup of the jet, such as periodic pulsating inlet pressure [12], electrohydrodynamic perturbation [13], mechanical vibration [11, 14], piezoelectric bending disk [15], oil-droplet chopper [16] and pneumatic micro-valve [17]. These active actuating methods require external actuation components, precise controlling of perturbation frequency, and/or complex microfabrication process. In addition, the relative position variations between the external force and microchannel result in a lower reproducibility and limit the parallelization of multi-channel [17]. Therefore, it is desirable to produce W/W droplets stably with no external perturbation.

Recently, passive microfluidic strategies are used to generate W/W droplets [18]. In passive methods, the critical point is to ensure that viscous shear and inertial forces are comparable or less than the interfacial tension force, which requires ultralow flow rates near or lower than the output limit of syringe pumps [18]. Conventional syringe pumps are inadequate for W/W droplet fabrication. To solve this issue, the hydrostatic pressure is introduced by inserting liquid-filled pipette tips into the inlets, and W/W droplets are generated passively [19, 20]. However, the hydrostatic pressure-driven method has two shortcomings: (1) The fluctuation of the hydrostatic pressure is inevitable due to the decrease in the liquid column height, and (2) the flow rates are prone to be affected by the surface characteristics of the microchannel (hydrophilic or hydrophobic), both of which vary the flow conditions and lower the uniformity and reproducibility. Kim et al. [21] used a pressure controller and a flow-board to control inlet pressures and flow rates simultaneously. W/W droplets are generated with variable size and high throughput. But double regulation of the pressure and flow rate also requires precise controlling components and complex feedback program, losing the

advantages of passive methods. To date, no simple, stable and controllable approach to passively produce W/W droplets exists. The main challenge in passive W/W droplets generation is to maintain ultralow flow rates in an inexpensive and stable manner.

Here, we present a simple and robust W/W droplet generation method on the basis of an evaporation pump with variable and ultralow flow rates. W/W droplets are generated uniformly and stably for nearly 1 h using poly (ethylene glycol) (PEG) and dextran (DEX) solutions as continuous and dispense phases, respectively. The influences of molecular weights, concentrations and flow rates are investigated systematically, and droplet production is scaled up by parallelizing eight droplet-formation units. Using the generated W/W droplets as microreactors, hydrogel particles are synthesized by either UV light or calcium ions, and recovered conveniently without removing oil phase.

Experimental

The fabrication of microdevices

A layer of dry film photoresist (the height was 120 μm) attached onto a clean glass slide. To eliminate the air, the photoresist was pressed by a roller uniformly and gently. Then, the photoresist was prebaked at 95 $^{\circ}\text{C}$ for 2 min, exposed by UV light for 14 s and baked again. After the development and washing, the remained photoresist pattern was placed in a 200 $^{\circ}\text{C}$ oven for 2 h, forming a positive mold. A mixture of polydimethylsiloxane (PDMS) monomer and curing reagent (10:1, v/v) was poured onto the fabricated positive mold, and the air was eliminated. After 3-h solidification, the PDMS layer was peeled off from the mold, and the reservoirs were punched. Then, we bonded the PDMS layer onto another clean glass slide by plasma.

The construction and the volumetric flow rate controlling of the evaporation pump

The evaporation pump was composed of an evaporation tube (EPt), a cache chamber, an output tube (OPt) and a sealing plug. EPt was polyvinyl chloride tubes with 0.8 mm inner diameters. The cache chamber and OPt were made of

polytetrafluoroethylene (PTFE). EPt, OPt and the cache chamber were connected with each other by two connectors. Ethyl acetate (EA) was filled in the system from one open end of EPt by a medical injector. When the whole system was filled up with EA, the open end of the OPt was placed in the DI water. Through pulling the medical injector, DI water was sucked into OPt and a water plug was generated in OPt. Then, we pulled out the medical injector and inserted the sealing plug. The evaporation pump was constructed completely and ready for use (Fig. S1A). To measure the volumetric flow rate, we recorded the time that liquid meniscus flew over a distance of 0.5 cm under microscopy, and calculated the volumetric flow rate. Based on this method, the flow rates of evaporation pumps with 0.05 cm, 0.2 cm, 0.5 cm and 1 cm EPts were measured, respectively.

W/W droplets generation

15% (w/v) PEG ($M_w = 500$ kDa) solution and 20% (w/v) DEX ($M_w = 20$ kDa) solution were added in wide-mouth bottles. In order to distinguish the PEG and DEX solutions, we added 0.1% (w/w) methylene blue into PEG solution. 0.8-mm polymer tubes were used to connect the bottles and the microdevice. The solutions were drawn into the microdevice and filled up all the channels by a medical injector. Then, we replaced the injector with the prepared evaporation pump with a 0.5-mm EPt. W/W droplets were generated at the flow-focusing junction stably.

The influence of concentration, molecular weight and flow rate on droplet size

To investigate the concentration effect, we used 500 kDa DEX and 20 kDa PEG to prepare 5% (w/v), 10% (w/v), 15% (w/v), 20% (w/v), 25% (w/v), 30% (w/v) DEX and PEG solutions, respectively. We chose a PEG solution as continuous phase and a DEX solution as disperse phase to form droplets, and took the photographs of flow pattern. Each PEG and DEX solution was tested one by one.

To evaluate the influence of DEX molecular weights, we prepared 20% (w/v) DEX solutions by using 500 kDa, 100 kDa and 40 kDa DEX. These DEX solutions with different molecular weights were used as disperse phase, and 20% (w/v) PEG (20 kDa) solution was used as continuous phase. The fluid was driven by the evaporation pump with a 0.3-mm EPt.

After droplets were generated stably, we took a movie of droplets and measured the size of 20 droplets in the movie.

Besides that, we fixed the concentrations of PEG and DEX at 15% (w/v) and 20% (w/v), respectively. The molecular weights of PEG and DEX were 20 kDa and 500 kDa. Then, we used the evaporation pump with a 0.3-mm EPt to drive the fluid, took a movie of droplets and calculated 20 droplets diameters. Following the same procedure, we investigate the flow pattern driven by the evaporation pumps with a 0.2 mm, 0.5 mm, 0.7 mm, 0.8 mm or 1.1 mm EPt.

The high-throughput production of W/W droplets

To produce droplets with a high throughput, we designed a three-dimensional (3-D) microdevice with 8 droplet-formation units. The fabrication of 3-D structures was described in elsewhere. The photograph of the 3-D microdevice was taken by a smartphone. In this 3-D microdevice, 20% DEX (500 kDa) and 20% PEG (20 kDa) solutions were sucked into the 3-D microchannel under the evaporation pump with a 2-cm EPt. Droplets were generated at all the flow-focusing junctions. Because the objective lens of our microscope cannot cover the whole microdevice, we captured the one image from the left side and another from the right side. The image of the whole microdevice was assembled by combing these two images. To observe the droplets clearly, we randomly captured images of two units under high-power lens.

The synthesis of hydrogel particles

The glycidyl methacrylate-modified DEX (DEX-GMA) was synthesized as follows: 10 g DEX (500 kDa) was dissolved in 90 mL DMSO. Under the protection of nitrogen, 2 g DMAP and 1.6 g GMA were added and reacted at 30 °C for 30 h. Then, the mixture was transferred into 400 mL ethanol dropwise. After standing and vacuum suction filtration, we obtained white precipitate. The white precipitate was resolved in 20 mL 4 °C DI water, and the pH was controlled in the range of 7–8. Then, this solution was dialyzed in DI water at 4 °C for 4 days. The product after dialysis was freeze-dried. The final white powder was DEX-GMA. By using 60% (w/v) DEX-GMA solution and 30% (w/v) PEG solution, DEX-GMA/

PEG droplets were generated in the 3-D microdevice and solidified into hydrogel particles by an ultraviolet (UV) source.

For Ca–alginate hydrogel particle synthesis, we designed a novel microdevice. 2.0% (w/v) sodium alginate was added into 20% (w/v) DEX solution to form dispersed phase. 5% (w/v) Ca^{2+} was dissolved in 30% (w/v) PEG solution to provide coordinating ions. DEX droplets containing sodium alginate were generated and reacted with Ca^{2+} in the downstream. The sodium alginate became Ca–alginate hydrogel. The synthesized DEX hydrogel and Ca–alginate hydrogel particles were recovered simply by DI water washing. Then the hydrogel particles were re-suspended in water to take white-field photograph and freeze-dried to capture SEM images.

Results and discussion

Principle of W/W droplet generation

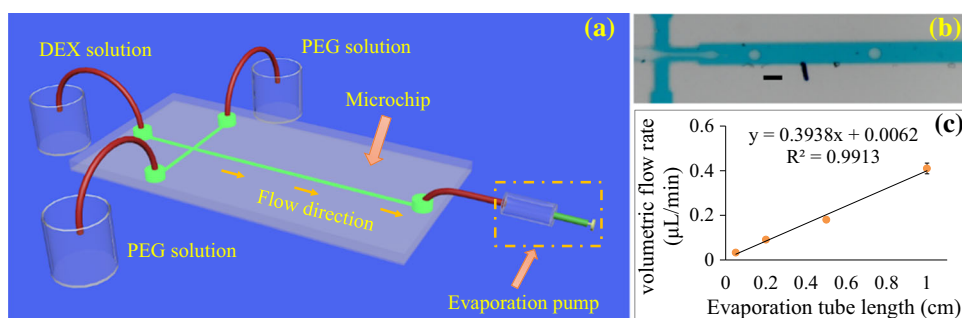
Figure 1a shows the setup of W/W droplets generation. A PDMS microdevice was fabricated through a modified soft lithography process. Then, 25% (w/v) PEG (500 kDa) and 20% (w/v) DEX (20 kDa) solutions were stored in wide-mouth bottles and connected to inlets, respectively. The outlet was connected to an evaporation pump with a 0.3-mm evaporation tube (EPT). Under the suction of the evaporation pump, PEG and DEX solutions flow into the microdevice and generated monodisperse W/W droplets stably at the flow-focusing region (Fig. 1b). For the passive generation of W/W droplets, the major issue is maintaining ultralow flow rates to break up the dispersed jet continuously. In this study, an evaporation pump was assembled by an EPT, a cache chamber, an output tube and a sealing plug to provide stable and ultralow flow rates (Fig. S1). The

system was filled with ethyl acetate (EA) and blocked by the sealing plug. EA in the EPT permeated the wall and diffused into the surrounding environment, reducing pressure in the system and generating a negative pressure at the open end of the output tube. The volumetric flow rate of the evaporation pump was determined by the EPT length. When the EPT length was changed from 500 μm to 1.0 cm, the volume flow rate of the output tube was increased from 0.033 to 0.41 $\mu\text{L}/\text{min}$, showing a good linear curve (Fig. 1b). This linear dependence relation provides us a flexible manner to control flow conditions in the microdevice.

Influence of PEG and DEX concentrations

For given molecular weights of PEG (500 kDa) and DEX (20 kDa), the concentration variations of PEG and DEX solutions lead to three flow patterns (Fig. 2a). In region I, the PEG and DEX solutions tended to form a three-layer laminar flow, because the interface tension was too small to support the breakup of DEX solution thread. In region II, W/W droplets were generated stably with high uniformity. In region III, W/W droplets were still formed, but the droplet size was not uniform. Some small daughter droplets following large droplets could be easily observed. As the volumetric flow rate of the evaporation pump was regulated flexibly in an ultralow range, the region of monodisperse W/W droplets (region II) was obviously larger than that in the previous methods [17]. In addition, the viscosity of continuous phase increased with the rising of PEG concentrations, which provides a reliable approach to adjust droplet size in the negative-pressure-driven model [22]. For example, the concentration of PEG solution was increased from 10% (w/v) to 30% (w/v). Correspondingly, the size of W/W droplets was varied in the range of 44–85 μm . The size distribution

Figure 1 a Schematic of W/W droplet generation setup. b Generated W/W droplets by using 15% (w/v) PEG and 20% (w/v) DEX solutions. Scale bar, 100 μm . c Flow rate regulation of the evaporation pump.



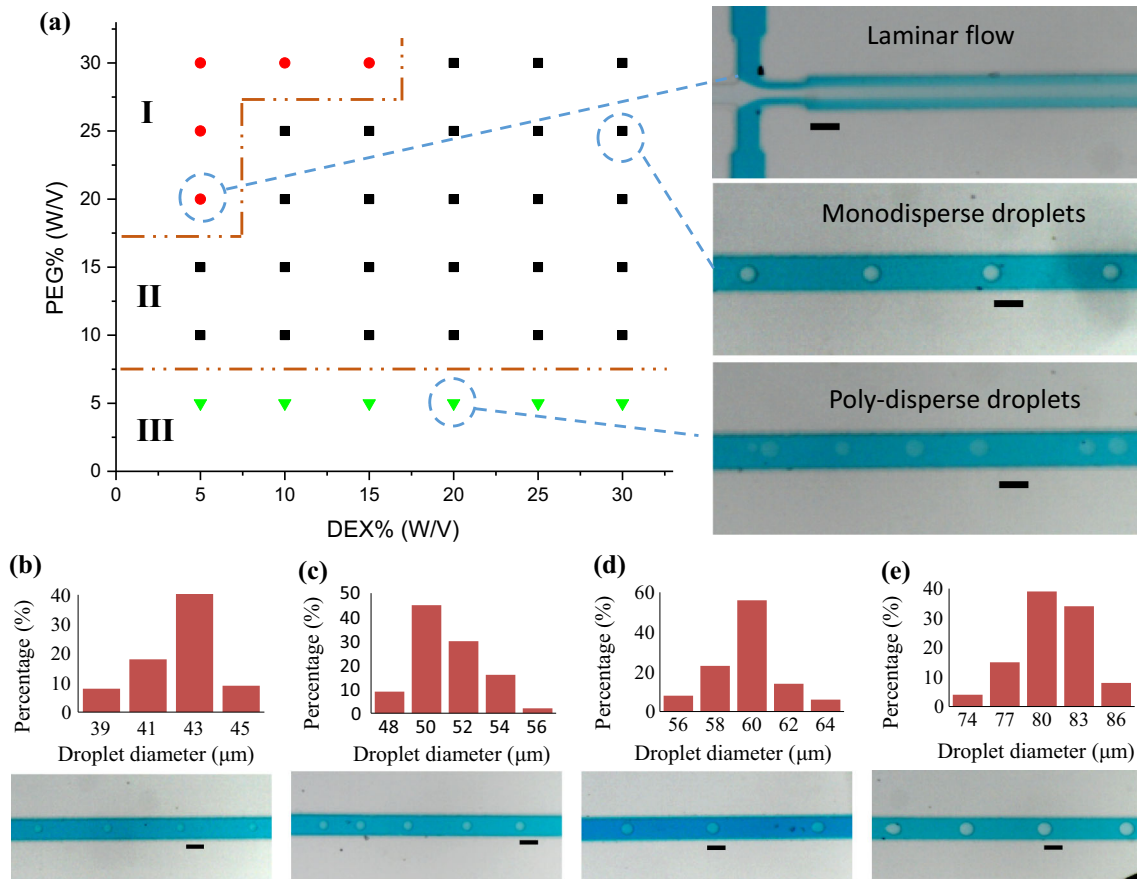


Figure 2 a Flow patterns under different PEG and DEX solutions. b–d Droplet size distributions by using 25% (w/v) DEX solution and 10% (w/v) (b), 15% (w/v) (c), 20% (w/v) (d), and 30% (w/v) (e) PEG solutions. Scale bars, 100 μm.

of droplets displayed Gaussian distribution (Fig. 2b–e).

Droplet size regulation through flow rate and DEX molecular weight

In positive-pressure-driven W/O droplet generation [23, 24], the droplet size was regulated flexibly and efficiently through varying the flow rates. However, all the solutions were driven by the same negative pressure source in our method. We could only change the whole output of the evaporation pump. The flow rates of PEG and DEX solutions could not be controlled independently. Therefore, the droplet size only showed small variations when the flow rate was changed from 0.018 to 0.034 μL/min (Fig. 3a). Once the flow rate was decreased to 0.014 μL/min, the DEX solution did not flow out of the junction (Fig. S2A). When the flow rate reached 0.038 μL/min, the DEX solution thread was prolonged, and non-uniform droplets were formed far from the junction

(Fig. S2B). To evaluate the influence of DEX molecular weight, we used 500, 100, and 40 kDa DEX to prepare 20% (w/v) DEX solutions, and 20 kDa PEG to prepare 20% (w/v) PEG solution. The results of droplet size distribution are shown in Fig. 3b. Under fixed concentrations, the molecular weight of DEX was smaller, and the W/W droplet size was larger, which was in accordance with a previous study [17]. The maximum droplet size reached 93 μm by using 40 kDa DEX. Of note, the interface tensions were reduced with the decrease in DEX molecular weight [10]. The reduced interface tension exacerbated the instability of droplet breakup. Thus, the variable coefficient (CV) of droplet size using 40 kDa DEX (5.2%) was poorer than that using 100 kDa (2.9%) and 500 kDa DEX (1.0%). In the next experiments, 500 kDa DEX was used.

Figure 3 Droplet size regulation by varying the flow rate of the evaporation pump (a) and the molecular weight of DEX (b). Scale bars, 100 μm .

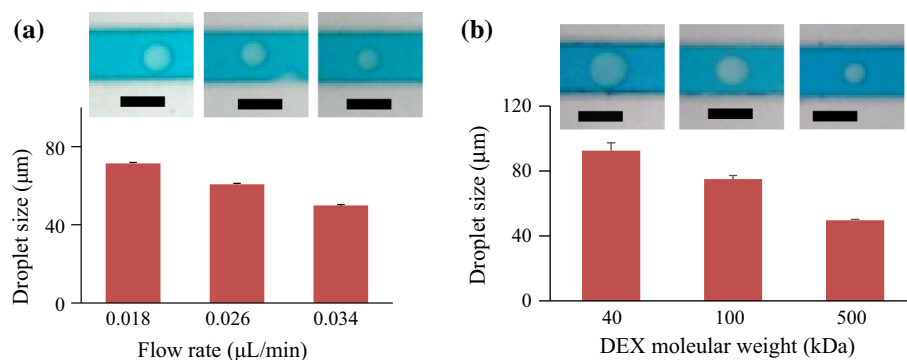
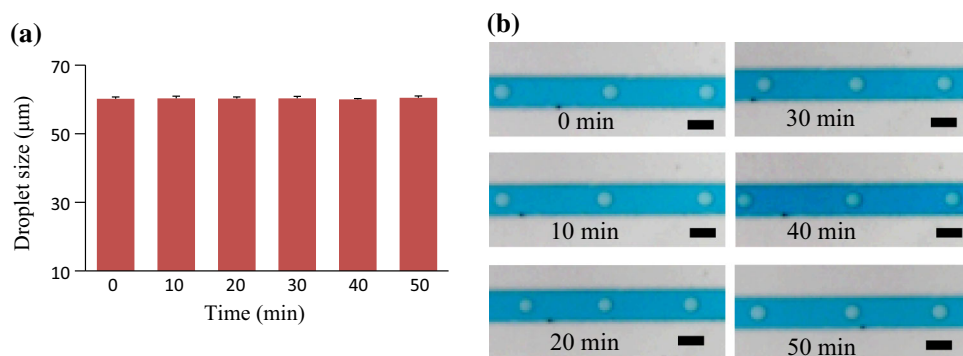


Figure 4 Stability of W/W droplet generation. **a** Statistical results of droplet size during 50 min of operation. **b** Bright-field images of W/W droplets at different time points. Scale bars, 100 μm .



Stability of the platform

In passive methods, the stability is an important parameter for end applications. The instability of the established method might result from the liquid level variation and the flow rate fluctuation of the evaporation pump. To eliminate the impact of liquid variations, PEG and DEX solutions were stored in wide-mouth bottles. For a limited time, the solution consumed by droplets did not result in a significant reduction in the liquid column in the bottles, which overcame the drawbacks of the hydrodynamic-pressure-driven passive method. Generally, solvent evaporation was affected by the temperature, humidity and evaporation areas. As the humidity in air is mainly induced by water vapor content, the quantity of EA molecules in air is not changed with the variation of the relative humidity. Thus, the humidity does not have obvious influence on the volume rate of the evaporation pump. Under room temperature (25 °C), the output of the evaporation pump could be maintained stably for several hours because the evaporation area was constant under the function of the cache chamber. In this case, we recorded W/W droplet generation for 50 min. The

droplet size showed a negligible fluctuation (Fig. 4), verifying the stability of this system.

Scaling-up of W/W droplet production

Another issue of W/W droplet is the small production. A possible approach to improve production is increasing the droplet-formation frequency or paralleling multi-channels. In this study, the droplet generation frequency is lower than that in active actuation methods. However, increasing the frequency still faces challenge. To offset the low frequency, we fabricated a 3-D microdevice with multi-channels (Fig. S3). The two inlets of the 3-D microdevice were connected to PEG and DEX solutions, respectively, and the outlet was connected to the evaporation pump with a 2-cm EPt (Fig. 5a). W/W droplets were generated at eight flow-focusing junctions simultaneously (Fig. 5b). The maximum frequency of single droplet-formation unit was 7–8 Hz. The total droplet production of the 3-D microdevice reached ~ 60 Hz, which was almost comparable with the active methods. The CV of droplet size in each unit changed from 2.4 to 2.9%. The whole CV for all eight units was 3.2%. The good

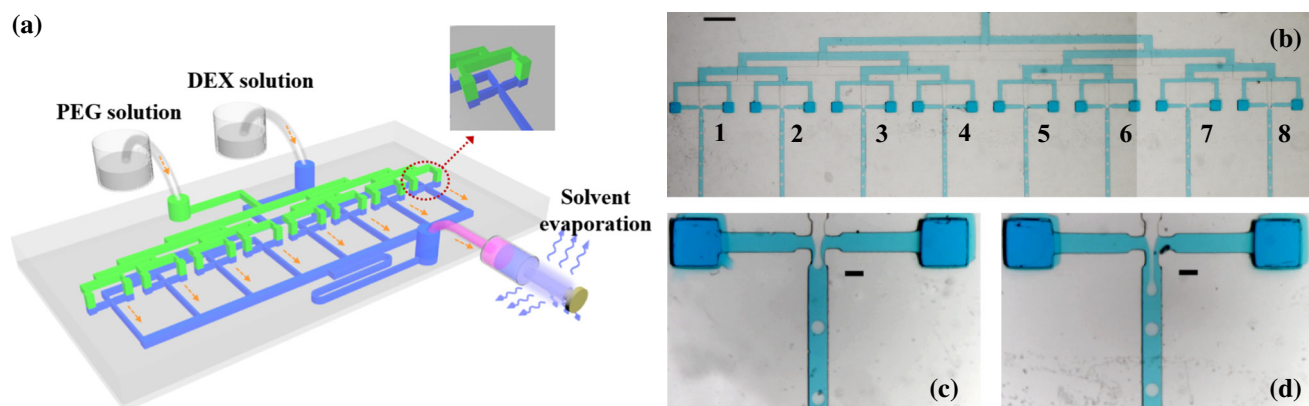


Figure 5 High-throughput generation of W/W droplets on a 3-D microdevice. **a** Schematic of the 3-D microdevice with eight droplet-formation units. Inset is the 3-D structure of flow-focusing

region. **b** Overall image of droplet generation in eight units. **c, d** Zoomed micrographs of two units. Scale bars, 100 μm .

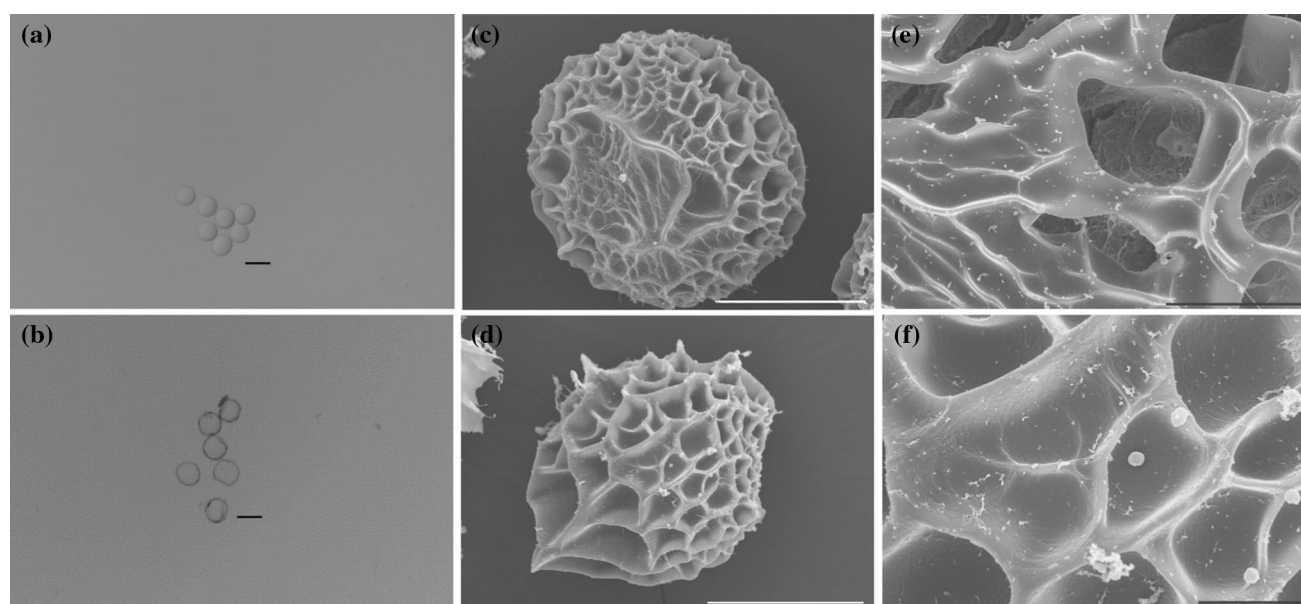


Figure 6 Synthesized hydrogel particles by using W/W droplets as reactors. **a, c** are bright-field and SEM photographs of DEX hydrogel particles. **b, d** Bright-field and SEM photographs of

calcium–alginate hydrogel particles. **e, f** Local magnification of porous structures. Scale bars, 100 μm (**a, b**), 30 μm (**c, d**), 10 μm (**e**) and 5 μm (**f**).

uniformity of droplets between different units indicated that the system stability was not influenced by the scaling-up processes (Fig. 5c, d). The 3-D structure reduced the inlets of fluids, simplified the fluid control and facilitated the integration of multi-channels. Thus, the production of droplets could be scaled up further by increasing the droplet-formation units.

Hydrogel particle synthesis

Compared with W/O droplets, W/W droplets contain no organic solvent. The recovery of encapsulated

molecules, particles and cells may be convenient without tedious post-treatment and washing processes. As an example, we used W/W droplets as microreactors to synthesize hydrogel particles. First, 15% (w/v) glycidyl methacrylate-modified DEX (DEX-GMA) and 20% (w/v) PEG solutions were used as disperse and continuous phases to form DEX-GMA/PEG droplets. Under UV initiation, the DEX-GMA/PEG droplets solidified into hydrogel spheres rapidly. The bright-field photograph verified that DEX hydrogel spheres were uniform (Fig. 6a). The

SEM image revealed that the hydrogel spheres had porous structure (Fig. 6c). The dimension of pores was several micrometers (Fig. 6e). Second, we added sodium alginate into the DEX solution with a final concentration of 1% (w/v). On an optimized microdevice (Fig. S4), calcium–alginate hydrogel particles were synthesized following an out-gelation process (Fig. 6b, d, f). Both DEX and calcium–alginate hydrogel particles were recovered easily, not requiring the removal of oil phase. The successful synthesis of UV-initiated or metal-ion-induced hydrogel particles verified that our method was efficient and suitable for various polymer materials.

Conclusions

In conclusion, we present a high-throughput and passive microfluidic platform to fabricate W/W droplets without requiring external perturbation. Under the suction of an evaporation micropump, W/W droplets are generated stably and uniformly for nearly 1 h. The droplet size is regulated in the range of 44–93 μm by changing the flow rate of the evaporation pump, the molecular weight of DEX and the concentration of PEG solution. On the 3-D microdevice, W/W droplets are fabricated in a high-throughput manner without significant loss of uniformity. The maximum frequency of droplet formation reaches ~ 60 Hz. Finally, DEX and calcium–alginate hydrogel spheres are synthesized successfully by UV initiation or calcium–ion coordination. The established method is simple, robust and suitable for various aqueous two-phase systems. The formed monodisperse W/W droplets are biocompatible vessels for biomolecules and cells, displaying a potential in drug carrier synthesis.

Acknowledgements

The authors are grateful to the Natural Science Foundation of China (NSFC 21575053, 21775057), the project of Six Talent Peaks (2017SWYY-013), “333” project of Jiangsu Province, The Natural Science Foundation of the Jiangsu Higher Education Institutions of China (16KJA150006), Postgraduate Research & Practice Innovation Program of Jiangsu Province (771231814).

Electronic supplementary material: The online version of this article (<https://doi.org/10.1007/s10853-019-04001-w>) contains supplementary material, which is available to authorized users.

References

- [1] Hardt S, Hahn T (2012) Microfluidics with aqueous two-phase systems. *Lab Chip* 12:434–442
- [2] Song Y, Shum HC (2012) Monodisperse w/w/w double emulsion induced by phase separation. *Langmuir* 28:12054–12059
- [3] Iqbal M, Tao Y, Xie S, Zhu Y, Chen D, Wang X, Huang L, Peng D, Sattar A, Shabbir MA, Hussain HI, Ahmed S, Yuan Z (2016) Aqueous two-phase system (ATPS): an overview and advances in its applications. *Biol Proced Online* 18:18
- [4] Sobrinos-Sanguino M, Zorrilla S, Keang CND, Monterroso B, Rivas G (2017) Encapsulation of compartmentalized cytoplasm mimic within lipid membrane by microfluidics. *Chem Commun* 53:4775–4778
- [5] Douliez JP, Martin N, Beneyton T, Eloi JC, Chapel JP, Navailles L, Baret JC, Mann S, Béven L (2018) Preparation of swellable hydrogel-containing colloidosomes from aqueous two-phase Pickering emulsion droplets. *Angew Chem Int Ed* 57:7780–7784
- [6] Zhang L, Cai LH, Lienemann PS, Rossow T, Polenz I, Vallmajo-Martin Q, Ehrbar M, Na H, Mooney DJ, Weitz DA (2016) One-step microfluidic fabrication of polyelectrolyte microcapsules in aqueous conditions for protein release. *Angew Chem Int Ed* 55:13470–13474
- [7] Lee TY, Ku M, Kim B, Lee S, Yang J, Kim SH (2017) Microfluidic production of biodegradable microcapsules for sustained release of hydrophilic actives. *Small* 13:1700646
- [8] Navi M, Abbasi N, Jeyhani M, Gnyawali V, Tsai SSH (2018) Microfluidic diamagnetic water-in-water droplets: a biocompatible cell encapsulation and manipulation platform. *Lab Chip* 18:3361–3370
- [9] Song Y, Sauret A, Shum HC (2013) All-aqueous multiphase microfluidics. *Biomicrofluidics* 7:061301
- [10] Helfrich MR, El-Kouedi M, Etherton MR, Keating CD (2005) Partitioning and assembly of metal particles and their bioconjugates in aqueous two-phase systems. *Langmuir* 21:8478–8486
- [11] Shum HC, Varnell J, Weitz DA (2012) Microfluidic fabrication of water-in-water (w/w) jets and emulsions. *Biomicrofluidics* 6:012808
- [12] Moon BU, Jones SG, Hwang DK, Tsai SS (2015) Microfluidic generation of aqueous two-phase system

- (ATPS) droplets by controlled pulsating inlet pressures. *Lab Chip* 15:2437–2444
- [13] Choi YH, Song YS, Kim DHJ (2010) Droplet-based microextraction in the aqueous two-phase system. *J Chromatogr A* 1217:3723–3728
- [14] Sauret A (2012) Forced generation of simple and double emulsions in all-aqueous systems. *Appl Phys Lett* 100:154106
- [15] Ziemecka I, van Steijn V, Koper GJ, Rosso M, Brizard AM, van Esch JH, Kreutzer MT (2011) Monodisperse hydrogel microspheres by forced droplet formation in aqueous two-phase systems. *Lab Chip* 11:620–624
- [16] Zhou C, Zhu P, Tian Y, Tang X, Shi R, Wang L (2017) Microfluidic generation of aqueous two-phase-system (ATPS) droplets by oil-droplet choppers. *Lab Chip* 17:3310–3317
- [17] Liu HT, Wang H, Wei WB, Liu H, Jiang L, Qin JH (2018) A microfluidic strategy for controllable generation of water-in-water droplets as biocompatible microcarriers. *Small* 14:e1801095
- [18] Mastiani M, Seo S, Jimenez SM, Petrozzi N, Kim MM (2017) Flow regime mapping of aqueous two-phase system droplets in flow-focusing geometries. *Colloid Surface A* 531:111–120
- [19] Moon BU, Abbasi N, Jones SG, Hwang DK, Tsai SS (2016) Water-in-water droplets by passive microfluidic flow focusing. *Anal Chem* 88:3982–3989
- [20] Moon BU, Hwang DK, Tsai SS (2016) Shrinking, growing, and bursting: microfluidic equilibrium control of water-in-water droplets. *Lab Chip* 16:2601–2608
- [21] Mastiani M, Seo S, Mosavati B, Kim M (2018) High-throughput aqueous two-phase system droplet generation by oil-free passive microfluidics. *ACS Omega* 3:9296–9302
- [22] Li HL, Xue YJ, Xu M, Zhao WF, Zong CH, Liu XJ, Zhang QQ (2017) Viscosity based droplet size controlling in negative pressure driven droplets generator for large-scale particle synthesis. *Electrophoresis* 38:1736–1742
- [23] Zhang QQ, Xu M, Liu XJ, Zhao WF, Zong CH, Yu Y, Wang Q, Gai HW (2016) Fabrication of Janus droplets by evaporation driven liquid–liquid phase separation. *Chem Commun* 52:5015–5018
- [24] Zhang QQ, Liu XJ, Liu DY, Gai HW (2014) Ultra-small droplet generation via volatile component evaporation. *Lab Chip* 14:1395–1400

Publisher's Note Springer Nature remains neutral with regard to jurisdictional claims in published maps and institutional affiliations.